J. Phys. Chem. A **2001,** *105,* 4118−4125

Perfluoroalkanes: Conformational Analysis and Liquid-State Properties from ab Initio and Monte Carlo Calculations

Edward K. Watkins and William L. Jorgensen*

Department of Chemistry, Yale University, New Haven, Connecticut 06520-8107

Received: November 7, 2000; In Final Form: January 31, 2001

Classical OPLS-AA force-field parameters are developed for perfluoroalkanes primarily by fitting to conformational profiles from gas-phase ab initio calculations (LMP2/cc-pVTZ(-f)//HF/6-31G*) and to experimental data for pure liquids. The ab initio C−C−C−C profile of *n*-C_4F_{10} (perfluorobutane) is similar to those from prior high-level calculations and indicates the presence of gauche (*g*) and ortho (*o*) minima and of anti (*a*) minima slightly offset from 180°. Ab initio torsional profiles for *n*-C_5F_{12} (perfluoropentane) and $(CF_3)_2CFCF_2CF_3$ (perfluoro-2-methylbutane) also show three sets of energy minima. Special OPLS-AA torsional parameters for these three molecules closely match ab initio and experimental geometries, conformational energies (ΔE_{min}), and conformational energy barriers. These specialized force fields were merged to provide a generalized force field for linear, branched, and cyclic perfluoroalkanes. The resultant parameters yield key ΔE_{min} values within 0.6 kcal/mol of the ab initio results for the three test compounds but more poorly represent the energy barriers. The parametrization also included reproduction of experimental liquid properties of these compounds, CF_4 (perfluoromethane) and *c*-C_5F_{10} (perfluorocyclopentane) via Monte Carlo (MC) simulations. MC simulations of six additional molecules were also performed in order to test the transferability of the force field.

Introduction

Perfluoroalkanes, perfluoroethers, and perfluoroamines (fluorous solvents) are being used increasingly in organic synthesis as substitutes for chlorinated solvents because they are nontoxic and do not deplete stratospheric ozone.[1−3] Furthermore, fluorous solvents are immiscible with both hydrocarbons and water,[1,4] which facilitates removal of organic product from the reaction medium via simple phase separation and filtration and also recycling of the solvent. These methods are often enhanced through the use of biphasic reactions in conjunction with recyclable catalysts that are soluble in the fluorous solvent because of perfluoroalkyl modification.[3,5] Supercritical carbon dioxide (CO_2) is another environmentally safe solvent that can be easily separated from organic reaction products. CO_2 solubilizes perfluorocarbons and perfluoroethers and, in parallel with fluorous solvents, is immiscible with hydrocarbons and water.[6,7] This has led to the development of surfactants with fluoroalkyl modification for such uses as dispersion polymerization[6] and the extraction of biomolecules.[7,8] Some of these surfactants are designed with branched fluorocarbon side chains,[8] presumably to promote packing of surfactant molecules for desired micelle shape, size, and phase orientation.

For medical applications, perfluoroalkanes and other fluorous liquids are used as oxygen-carrying blood substitutes.[9,10] Liquid and gaseous perfluoroalkanes are used as high-density intraoperative fluids for eye surgery.[10,11] When emulsified to microbubbles, gaseous perfluoropropane is used as an ultrasound contrast agent to detect myocardial perfusion abnormalities.[12] This application benefits from the high density, the low blood solubility, and the low blood diffusivity of C_3F_8. Thus, fluorous fluids are important to medical applications, and fluorous fluids and solutes containing fluoroalkyl modification are important to organic synthesis and separation methods.

Parallel computational studies are desirable, and in view of the emphasis on the liquid state, tractable approaches are molecular dynamics (MD) or Monte Carlo statistical mechanics (MC) simulations with classical force fields. The conformational analysis of perfluoroalkanes is intriguing. The presence of three pairs of enantiomeric energy minima for the C−C−C−C torsional profile of *n*-C_4F_{10} is well-established based on ab initio calculations[13−18] and on N_2 matrix-isolation IR spectroscopy.[13−15] The gauche conformers (g_+, g_-) have CCCC dihedral angles ca. 60° and −60°. The ortho or orthogonal conformers (o_+, o_-) have dihedral angles near 90° and −90°. Finally, the anti conformers (a_+, a_-) have dihedral angles on either side of the trans angle of 180°. The trans conformer represents a low energy barrier between the a_+ and a_- global minima. Ab initio calculations for other *n*-A_4X_{10} systems yield similar profiles,[15,19] and an electron diffraction study of *n*-Si_4Me_{10} established the presence of *a* and *g* minima and the “probable” presence of *o* minima.[19] A six-conformer rotational isometric state (RIS) model for poly(tetrafluoroethylene) (PTFE) best simulates experimental data with matrix terms incorporating the g_+, g_-, o_+, o_-, a_+, and a_- conformers, although a four-state model that merges the g_+ and o_+ conformers and the g_- and o_- confomers performs nearly as well.[16] Another RIS model, derived from neutron diffraction data of PTFE, also supports the existence of *g*, *o*, and *a* minima (see Figure 3 of ref 20 and Figure 6 of ref 21).

Previous force-field efforts for perfluoroalkanes have primarily focused on modeling linear PTFE.[17,22−27] Jaffe and coworkers briefly described force fields for linear, branched, and

---

* To whom correspondence should be addressed.

10.1021/jp004071w CCC: $20.00

cyclic perfluoroalkanes, but the basis set for parameter development only consisted of linear molecules.[28,29] Dixon and co-workers developed spectroscopic force fields for linear, branched, and cyclic perfluoroalkanes and perfluoroethers,[30] but their parameters have little transferability to condensed media. The force-field studies of Kollman and co-workers[31] and of Yamamoto and co-workers[32] were limited to CF_4 and C_3F_8, respectively, whereas Cummings and co-workers[33] and Sprik and co-workers[27] developed united-atom force fields rather than all-atom (AA) models.

Many groups have noted the complexity of torsional energetics for perfluoroalkanes. Allinger and co-workers used a standard V_1 to V_3 three-term Fourier series but state the need for a V_6 term.[18] Rosi-Schwartz and Mitchell presented both a four-term Fourier series for PTFE[24] and a more refined seven-term series.[25] Okada and co-workers presented a six-term Fourier series and also introduced extra terms for 1,5-nonbonded F−F interactions to obtain the *a* conformers as the global minima.[17]

In the present paper, classical AA force-field parameters specific to n-C_4F_{10}, n-C_5F_{12}, and $(CF_3)_2CFCF_2CF_3$ and generalized parameters for all linear, branched, and cyclic perfluoroalkanes are developed within the OPLS (optimized potentials for liquid simulations) framework.[34] As usual, the development considers molecular structures, conformational energetics, and pure liquid properties. The parameter development has extended the conformational analysis of perfluoroalkanes through computation of ab initio energy profiles for linear n-C_4F_{10} and n-C_5F_{12} and for branched $(CF_3)_2CFCF_2CF_3$. In addition, the first extensive simulation studies of perfluoroalkane liquids have been carried out. This included results for CF_4, n-C_4F_{10}, n-C_5F_{12}, $(CF_3)_2CFCF_2CF_3$, and c-C_5F_{10} during parameter development, followed by testing for six additional liquids.

Computational Methods

Force Field and Parametrization. The potential energy function consists of harmonic bond stretching and angle bending terms, a Fourier series for torsional energetics, and Coulomb and Lennard-Jones terms for the nonbonded interactions, eqs 1−4.[34] The parameters are the force constants k, the r_0 and ϑ_0 reference values, the Fourier coefficients V, the partial atomic charges q, and the Lennard-Jones radii and well-depths, σ and ϵ.

$$E_{\text{bond}} = \sum_i k_{b,i}(r_i - r_{0,i})^2 \tag{1}$$

$$E_{\text{bond}} = \sum_i k_{\vartheta,i}(\vartheta_i - \vartheta_{0,i})^2 \tag{2}$$

$$E_{\text{torsion}} = \sum_i \left[\frac{1}{2}V_{1,i}(1 + \cos\varphi_i) + \frac{1}{2}V_{2,i}(1 - \cos 2\varphi_i) + \frac{1}{2}V_{3,i}(1 + \cos 3\varphi_i) + \frac{1}{2}V_{4,i}(1 - \cos 4\varphi_i)\right] \tag{3}$$

$$E_{\text{nonbond}} = \sum_i \sum_{j>i} \left\{\frac{q_i q_j e^2}{r_{ij}} + 4\epsilon_{ij}\left[\left(\frac{\sigma_{ij}}{r_{ij}}\right)^{12} - \left(\frac{\sigma_{ij}}{r_{ij}}\right)^{6}\right]\right\} \tag{4}$$

Standard combining rules are used such that $\sigma_{ij} = (\sigma_{ii}\sigma_{jj})^{1/2}$ and $\epsilon_{ij} = (\epsilon_{ii}\epsilon_{jj})^{1/2}$.[34] The nonbonded interactions are evaluated intermolecularly and for intramolecular atom pairs separated by three or more bonds. The 1,4-intramolecular interactions are reduced by a factor of 2 in order to use the same parameters for both intra- and intermolecular interactions.[34]

Standard bond stretching and angle bending parameters were initially assigned from the OPLS-AA parameter set,[34] which includes some entries from the AMBER AA force field.[31,35] Each atom has an associated two-letter atom type that is used to designate the parameters for atom pairs (bond stretching) or atom triplets (angle bending). The atom types used here are CT (aliphatic sp^3 carbon) and F (fluorine).

The present work then focused on the development of the Fourier coefficients, partial charges, and Lennard-Jones parameters in an iterative process. First, a Z matrix was constructed for each perfluoroalkane, and initial parameters were assigned based on the published values.[31,34,35] Trial partial charges were estimated to be self-consistent within the OPLS-AA framework on the basis of the relative electronegativities of the elements. We settled on a partial charge of −0.12 e for fluorine; however, MC simulations for liquid perfluoroethane with constant Lennard-Jones parameters showed changes of less than 1% for the computed density and heat of vaporization with flourine charges of −0.10 to −0.16 e. Both quantities decrease slightly with the higher charge magnitude. Gas-phase energy minimizations were then performed with the BOSS program[36] with these parameters. The geometries obtained were compared with those from experiments and from ab initio optimizations at the HF/6-31G* level. This provided a basis for adjusting the parameters for bond stretching and angle bending. All ab initio calculations were performed with Jaguar[37] on a Silicon Graphics Indigo2 with an R10000 processor.

The procedure for establishing missing Fourier coefficients has been described.[34] The F−CT−CT−F and CT−CT−CT−F parameters were developed based on experimental and ab initio torsional profiles of C_2F_6,[38−40] of C_3F_8,[41] and of selected hydrofluoroalkanes. For determining CT−CT−CT−CT parameters, energy scans were performed with LMP2/cc-pVTZ(-f)//HF/6-31G* calculations.[42,43] Calculations at this level are known to have striking accuracy for conformational energetics with average errors of 0.25 kcal/mol for the Halgren test set.[42,43] The scans were performed at 10° intervals for the CCCC dihedral of n-C_4F_{10} and for the C4C3C2F dihedral of $(CF_3)_2CFCF_2CF_3$. For n-C_5F_{12}, one CCCC dihedral was scanned while the other CCCC dihedral angle was fixed at 180°. Full optimizations were done at each point with the exception of the chosen dihedral angles. Similarly, the same energy scans were carried out using the force field with the BOSS program and with the Fourier coefficients for all CT-CT-CT-CT torsions set to zero. For the Fourier coefficients specific to n-C_4F_{10}, n-C_5F_{12}, and $(CF_3)_2CFCF_2CF_3$, the relative energies from the scans were used as input to the Simplex-based fitting program, Fit,[44] to determine the Fourier coefficients that minimize the differences between the LMP2/cc-pVTZ(-f)//HF/6-31G* and force-field results.

The generalized CT−CT−CT−CT Fourier coefficients for perfluoroalkanes were designed to reproduce the energy differences between conformational energy minima, ΔE_{min}, from the LMP2 calculations. Three additional steps were performed to establish these coefficients. First, using the method described for the specific coefficients, V_1 to V_4 coefficients were determined that gave the best overall fit for all data points for the three compounds. Second, the coefficients were further refined by selectively excluding from consideration high-energy conformers for the three compounds; the V_1 from these iterations was used as the generalized V_1 coefficient, and the V_2 to V_4 coefficients were the basis for further fitting. Third, the Fit

TABLE 1: Ab Initio and Experimental C−C−C−C Torsional Data for *n*-C_4F_{10}[a]

		eclipsed	gauche	gauche to ortho	ortho	ortho to anti	anti	trans
LMP2/cc-pVTZ(-f)//	**angle**	**0**	**54**	**81**	**98**	**120**	**170**	**180**
HF/6-31G*[b]	Δ*E*	7.8	0.8	2.1	1.9	2.4	0.0	0.1
HF/6-31G*[c]	**angle**	**0**	**56**	**83**	**96**	**120**	**169**	**180**
	Δ*E*	8.5	1.2	2.3	2.0	2.7	0.0	0.1
MP2/6-31G*[d]	**angle**		**54**		**95**		**166**	
	Δ*E*		0.7		1.6		0.0	
MP2/6-311G*[d]	Δ*E*		0.9		2.1		0.0	
HF/D95+*[e]	**angle**		**56**		**95**		**167**	**180**
MP2/D95+*[e]	Δ*E*		0.5		1.7		0.0	0.2
HF/6-31G[f]	Δ*E*				1.6	2.5	0.0	0.2
MP2/6-31G*[g]	Δ*E*		0.7		1.6		0.0	
MP2/DZ+P[h]	Δ*E*	8.0	1.5			2.4	0.0	0.4
exptl (gas)[i]	Δ*E*		1.2					
exptl (N_2 matrix)[d]	Δ*E*		ca. 0.9					

[a] Angles in deg, Δ*E* in kcal/mol relative to the anti conformer. [b] This work, based on a spline fit to the ab initio data taken at 10° intervals. [c] Reference 15. [d] Reference 14. [e] Reference 16. [f] Reference 17. [g] Reference 18. [h] Reference 53. [i] References 53−56.

program was used in an iterative process to adjust the V_2 to V_4 coefficients to minimize the differences between the ab initio and force-field results for the lowest-energy minima. The V_3 coefficient was successively fit to the 70°−20° $\Delta E_{\min}$ for $(CF_3)_2CFCF_2CF_3$, whereas the V_2 and V_4 coefficients were successively fit to the 170°−50° $\Delta E_{\min}$ for *n*-C_4F_{10} and *n*-C_5F_{12} and to the 70°−170° $\Delta E_{\min}$ for $(CF_3)_2CFCF_2CF_3$.

The Fourier coefficients, for both the specific and the generalized cases, often required refitting when atomic charges, Lennard-Jones parameters, or both are subsequently adjusted. When satisfactory agreement with molecular structures and torsional energy scans were obtained, MC simulations for the five pure liquids were performed. Some adjustments of the Lennard-Jones parameters were made so that calculated properties for the pure liquid perfluoralkanes agreed well with experiment. Because our efforts were guided by consideration of multiple types of experimental and ab initio data, the final parameter set reflects a compromise.

Pure Liquid Simulations. The Metropolis MC simulations[45] were performed with the BOSS program on Silicon Graphics workstations or a multiprocessor Pentium cluster running Linux. All molecules were fully flexible, i.e., the sampling included bond stretching, angle bending, and torsional motion in addition to the total translations and rotations. This necessitates that MC simulations be performed for both the ideal gas and the liquids in order to compute heats of vaporization, ΔH_{vap}. The calculations were executed with the generalized force field in the NPT ensemble, preferably at a pressure and temperature where experimental data are available for both liquid density and ΔH_{vap}. For most systems, this was 1 atm and either the normal boiling point of the liquid or near 25 °C. Gas-phase simulations consisted of 3 million (3M) configurations of equilibration, followed by 3M configurations of averaging, which were run in batches of 0.6M configurations. For the pure liquids, periodic boundary conditions were employed with cubic cells of 267 molecules. The equilibrated box sizes ranged from approximately 29 × 29 × 29 Å for CF_4 to 45 × 45 × 45 Å for *n*-C_6F_{14} (perfluorohexane). For the cutoff of intermolecular nonbonded interactions, a residue-based approach was taken; basically, if any C−C distance was below 12 Å, the entire molecule−molecule interaction was included, and a standard correction was made for Lennard-Jones interactions neglected beyond the cutoff.[46] Each liquid was first equilibrated for 8M configurations, and the averaging occurred over an additional 5M configurations, which were run in batches of 0.5M configurations. Statistical uncertainties (±1σ) were obtained through the batch means procedure (eq 5), where m is the number of batches and θ_i is the average of property θ in the ith batch.[46]

$$\sigma^2 = \sum_i^m (\theta_i - \langle\theta\rangle)^2/m(m-1) \tag{5}$$

The computed densities, heats of vaporization, radial distribution functions, energy distributions, and conformational properties are very well converged with MC simulations of this length. By adjusting the allowed ranges for rigid-body rotations, translations, and dihedral angle movement, acceptance rates averaged ca. 30% for new configurations. The ranges for bond stretching and angle bending are set automatically by the BOSS program on the basis of the force constants and temperature.

Results and Discussion

Ab Initio Profiles. Prior ab initio and experimental data for the CCCC torsional profile of *n*-C_4F_{10} are summarized in Table 1, along with the present LMP2/cc-pVTZ(-f)//HF/6-31G* results. Some references report ab initio calculations at several levels of theory; only the highest-level results with the most complete data are noted in Table 1. The reported angles and Δ*E* values for the LMP2/cc-pVTZ(-f)//HF/6-31G* set are based on a spline fit to the profiles with the 10° increments. For *n*-C_4F_{10}, the ab initio results in Table 1 are in close accord. All angles agree within 4°, and all energies agree within 0.7 kcal/mol. The *g* conformers are energy minima, the *a* conformers are the global minima, and the trans energy barrier is in the range of 0.1−0.4 kcal/mol. The *o* minima are reported in all studies except for the MP2/DZ+P one, though it is unclear if the ortho regions were examined. The experimental values for the *a* to *g* $\Delta E_{\min}$ (Table 1) are ca. 1.0 kcal/mol, which is similar to most of the ab initio results.

The present LMP2 torsional energy profiles for *n*-C_4F_{10}, *n*-C_5F_{12}, and $(CF_3)_2CFCF_2CF_3$ are plotted in Figures 1−3, along with the OPLS-AA profiles, which are discussed below. The CCCC LMP2 profiles for *n*-C_4F_{10} (Figure 1) and *n*-C_5F_{12} (Figure 2) are similar; both compounds have *g*, *o*, and *a* minima at approximately the same angles, and both have similar $\Delta E_{\min}$ and the same torsional energy barriers. The C4C3C2F LMP2 profile for $(CF_3)_2CFCF_2CF_3$ (Figure 3) also shows three enantiomeric pairs of minima at ca. 20°, 70°, and 170°.

In a key study, Michl and co-workers provide a formalism to explain the occurrence of three pairs of enantiomeric minima for certain *n*-A_4X_{10} molecules.[15] Their model largely focuses

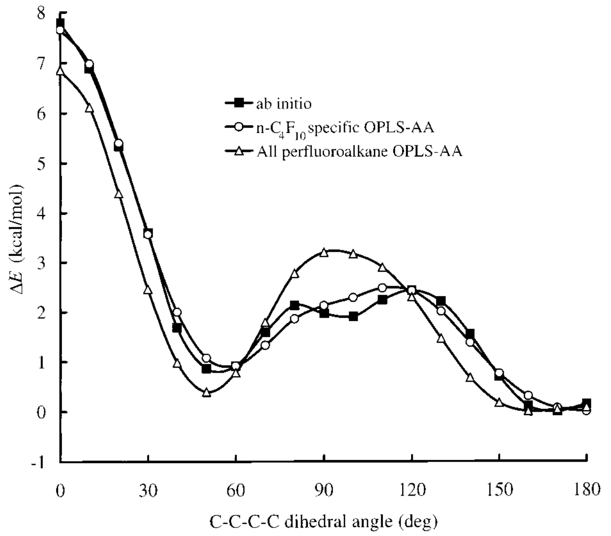

Figure 1. ΔE vs CCCC dihedral angle for n-C_4F_{10} from LMP2/cc-pVTZ(-f)//HF/6-31G* calculations, n-C_4F_{10} specific OPLS-AA force-field calculations, and generalized perfluoroalkane OPLS-AA force-field calculations.

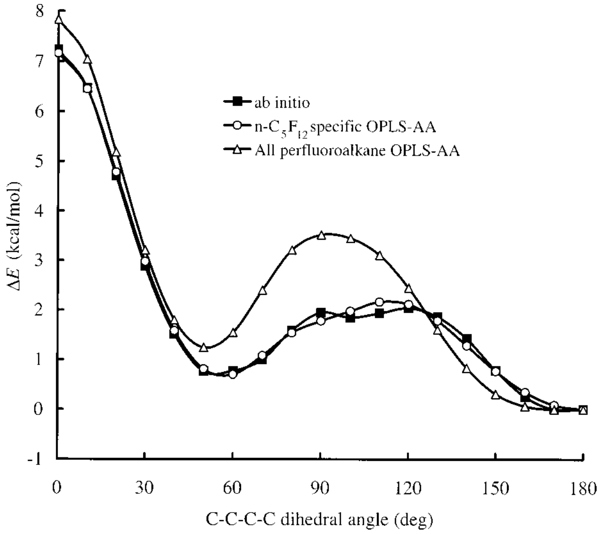

Figure 2. ΔE vs CCCC dihedral angle for n-C_5F_{12} from LMP2/cc-pVTZ(-f)//HF/6-31G* calculations, n-C_5F_{12} specific OPLS-AA force-field calculations, and generalized perfluoroalkane OPLS-AA force-field calculations. The second CCCC dihedral is held fixed at 180°.

on an interplay between steric hindrance, as described by van der Waals interactions, and molecular-orbital-based antiperiplanar stabilization. Charge−charge interactions have only minor importance, although the authors acknowledge that Coulombic forces could play a role in alternative formalisms. The optimized HF/6-31G* geometries nearest the minima and maxima for n-C_4F_{10} are illustrated in Figure 4. In going from a *g* minimum (4a), to a *g*−*o* transition structure (4b), to an *o* minimum (4c), the 1,6-FF interaction shown with asterisks provides the greatest steric repulsion at the transition structure (4b). The staggering of the substituents for an alkane-like gauche minimum causes the fluorines with the asterisks to be too close; the repulsion is relieved and the *g* and *o* minima arise by twisting the CCCC angle in either direction, while simultaneously twisting the terminal CF_3 groups clockwise and counterclockwise, respectively. Antiperiplanar forces stabilize the all-staggered trans maximum (4e), but 1,5-FF interactions (shown with pound symbols) produce a small torsional offset to an *a* minimum (4d).

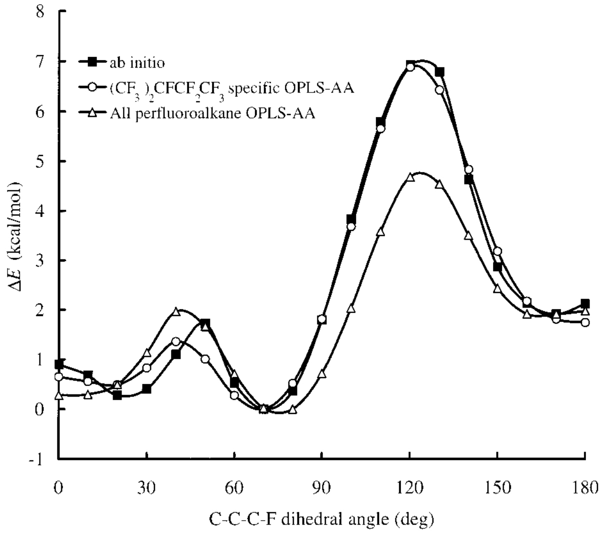

Figure 3. ΔE vs C4C3C2F dihedral angle for $(CF_3)_2CFCF_2CF_3$ from LMP2/cc-pVTZ(-f)//HF/6-31G* calculations, $(CF_3)_2CFCF_2CF_3$ specific OPLS-AA force-field calculations, and generalized perfluoroalkane OPLS-AA force-field calculations.

Force-Field Parameters. The final OPLS-AA parameters for perfluoroalkanes are reported in Tables 2−5. The bond stretching and angle bending parameters (Tables 2 and 3) are from prior work. As before,[34,47] the molecular structures from OPLS-AA optimizations are essentially identical to HF/6-31G* and experimental results;[18,38,48,49] for bond lengths and bond angles, the average deviations are 0.01 Å and 1°.

The nonbonded parameters for perfluoroalkanes are listed in Table 4. The partial charge on fluorine was fixed at $-0.12\ e$, and the partial charge on carbon becomes more positive by 0.12 e with increased fluorine substitution. The Lennard-Jones parameters remain unchanged from the original OPLS-AA parameter set[34] with minor exceptions. The ϵ was adjusted for CT in CF_4 and both ϵ and σ were adjusted for F to obtain satisfactory agreement with both the experimental densities and heats of vaporization of pure liquids. Otherwise, the Lennard-Jones parameters for CT in all perfluoroalkanes are the same with $\sigma = 3.50$ Å and $\epsilon = 0.066$ kcal/mol. Basically, there were only four adjusted parameters, the q, σ, and ϵ for fluorine plus the ϵ for CF_4. It is notable that the small number of unique parameters in Table 4 works so well for the predicted liquid properties of the present structurally diverse perfluoroalkanes (Table 6).

The torsional parameters are listed in Table 5. The compound-specific OPLS-AA parameters reproduce the CCCC ab initio LMP2 torsional-energy profiles with average differences of 0.2 kcal/mol for n-C_4F_{10}, 0.1 kcal/mol for n-C_5F_{12}, and 0.2 kcal/mol for $(CF_3)_2CFCF_2CF_3$. For n-C_4F_{10} (Figure 1) and n-C_5F_{12} (Figure 2), the gauche torsional angle of ca. 50° is reproduced, but the trans conformers become the global minima, and the nearby *a* minima are lost. Even though the compound-specific force-field curves for n-C_4F_{10} and n-C_5F_{12} are quite flat in the *o* regions, the shallow *o* minima at ca. 100° are not reproduced. The LMP2 calculations show that the *a* and *o* minima have barriers of less than 0.4 kcal/mol for interconversion to other conformers. The compound-specific OPLS-AA parameters for $(CF_3)_2CFCF_2CF_3$ (Figure 3) reproduce the ab initio minimum at ca. 70°, but shift the ca. 20° minimum to 0° and the ca. 170° minimum to 180°.

The generalized OPLS-AA parameters reproduce the ab initio torsional-energy profiles with average differences of 0.6 kcal/

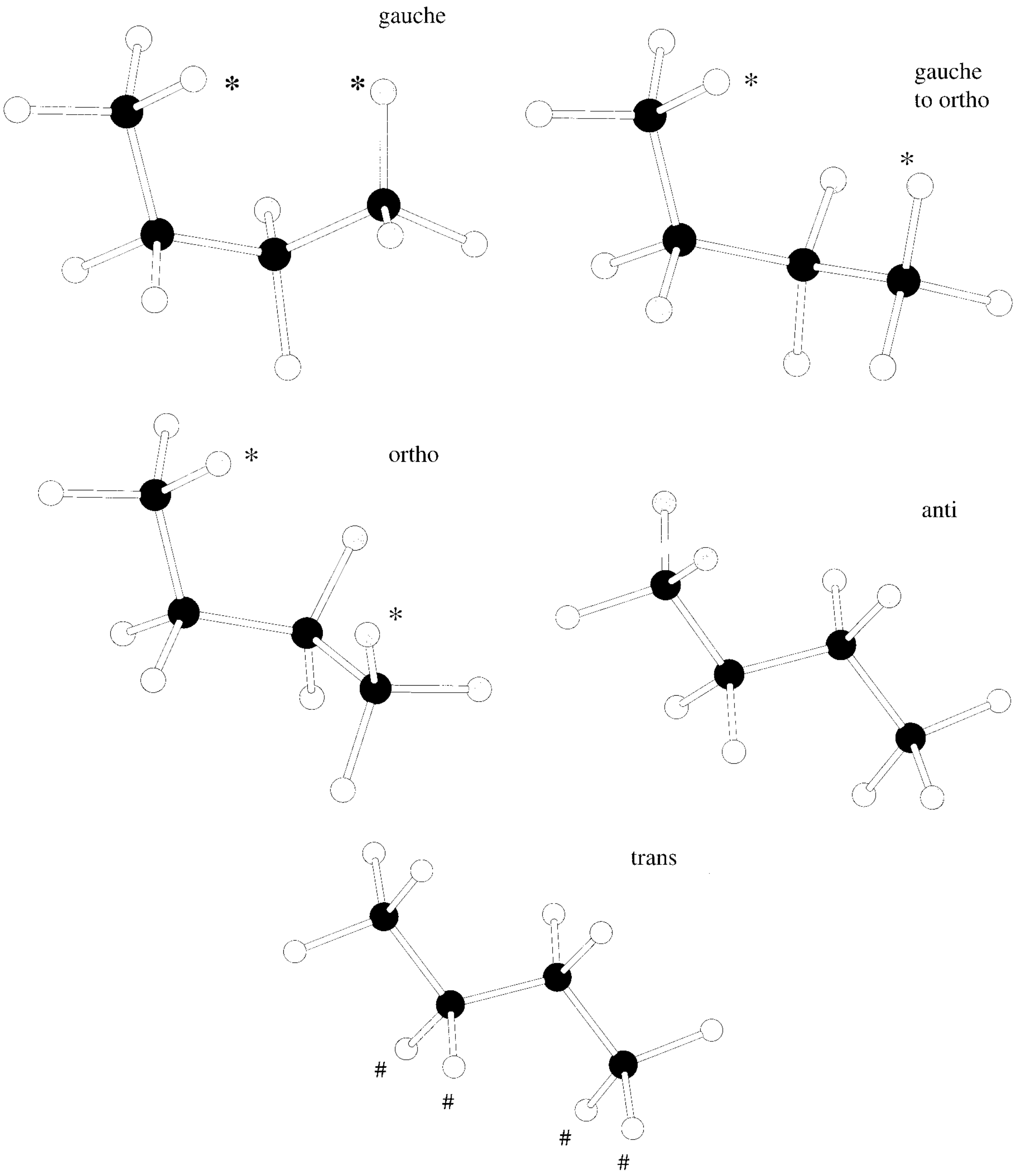

Figure 4. HF/6-31G* geometries nearest the minima and maxima of n-C_4F_{10}: (a) g minimum, (b) g−o transition structure, (c) o minimum (asterisks indicate 1,6 steric interaction), (d) a minimum, (e) trans maximum (pound signs indicate 1,5 steric interactions).

TABLE 2: OPLS-AA Bond Stretching Parameters for Perfluoroalkanes

bond	k_b (kcal mol^{-1} Å^{-2})	r_0 (Å)
CT−F[a]	367.0	1.332
CT−CT[b]	268.0	1.529

[a] Reference 31. [b] Reference 34.

mol for n-C_4F_{10} (Figure 1), 0.7 kcal/mol for n-C_5F_{12} (Figure 2), and 0.8 kcal/mol for $(CF_3)_2CFCF_2CF_3$ (Figure 3). The a minima now correctly reappear for in all cases. Furthermore, the generalized parameters reproduce the key energy differences within a few tenths of a kcal/mol. These are the 170°−50° $\Delta E_{\min}$ for n-C_4F_{10} and n-C_5F_{12} and the 70°−20° and the 70°−170° $\Delta E_{\min}$ for $(CF_3)_2CFCF_2CF_3$. The downside is that the g to a barrier heights are less well reproduced.

TABLE 3: OPLS-AA Angle Bending Parameters for Perfluoroalkanes

angle	k_θ (kcal mol^{-1} rad^{-2})	θ_0 (deg)
F−CT−F[a]	77.00	109.10
CT−CT−F[b]	50.00	109.50
CT−CT−CT[c]	58.35	112.70

[a] Reference 35. [b] Reference 57, same as CT−CT−OH and CT−CT−OS in Reference 35. [c] Reference 34.

As suggested by other studies,[17,18,25] the introduction of Fourier terms with higher periodicities could be helpful, but they are not normally included in MD and MC calculations.

Pure Liquid Results. The OPLS-AA parameters for CF_4, n-C_4F_{10}, c−C_5F_{10}, n-C_5F_{12}, and $(CF_3)_2CFCF_2CF_3$ were developed in conjunction with computation of their liquid densities and heats of vaporization. These are important properties

TABLE 4: OPLS-AA Nonbonded Parameters for Perfluoroalkanes

atom type	atom or group	q (e^-)	σ (Å)	ϵ (kcal mol^{-1})
F	F	−0.12	2.95	0.053
CT	CF_4	0.48	3.50	0.097
CT	CF_3 group	0.36	3.50	0.066
CT	CF_2 group	0.24	3.50	0.066
CT	CF group	0.12	3.50	0.066

TABLE 5: OPLS-AA Fourier Coefficients (kcal mol^{-1}) for Perfluoroalkanes

dihedral angle	V_1	V_2	V_3	V_4
	General			
F−CT-CT-F	−2.500	0.000	0.250	0.000
CT-CT-CT-F	0.300	0.000	0.400	0.000
CT-CT-CT-CT	6.622	0.948	−1.388	−2.118
	n-C_4F_{10} Specific			
CT-CT-CT-CT	7.219	−0.484	−1.105	−0.990
	n-C_5F_{12} Specific			
CT-CT-CT-CT	5.829	−0.453	−1.266	−1.052
	$(CF_3)_2CFCF_2CF_3$ Specific			
CT-CT-CT-CT	8.227	−0.106	−0.435	−1.676

because they reflect both the sizes of the molecules and the average intermolecular interactions. The transferability of the generalized parameters was tested through subsequent MC simulations for the pure liquids of C_2F_6 (perfluoroethane), C_3F_8, c-C_4F_8 (perfluorocyclobutane), n-C_6F_{14}, $(CF_3)_2CF(CF_2)_2CF_3$ (perfluoro-2-methylpentane), and $(CF_3)_2(CF)_2(CF_3)_2$ (perfluoro-2,3-dimethylbutane). The results are shown in Table 6. In all cases, excellent agreement with experimental densities was obtained with an average unsigned error of 1%.

Heats of vaporization are readily computed from the simulation results using eq 6.

$$\Delta H_{\mathrm{vap}} = \Delta H_{\mathrm{gas}} - \Delta H_{\mathrm{liquid}} = E_{\mathrm{intra}}(\mathrm{gas}) - E_{\mathrm{tot}}(\mathrm{liq}) + RT \quad (6)$$

Here, E_{intra}(gas) is the average intramolecular energy in the gas phase and E_{tot} (liq) is the total potential energy of the liquid consisting of both the average intramolecular energy of the liquid, E_{intra}(liq), and the average intermolecular energy of the liquid, E_{inter}(liq). The PV-work term in the enthalpy is equal to RT for the ideal gas and it is negligible for the liquid. The heats of vaporization obtained from the MC simulations for the gases and liquids are also in good agreement with the experimental data in Table 6; the average unsigned error is less than 3%.

Intermolecular radial distribution functions (rdfs) provide a measure of the local structure in liquids, and coordination numbers can be obtained by the integration of their peaks.[46]

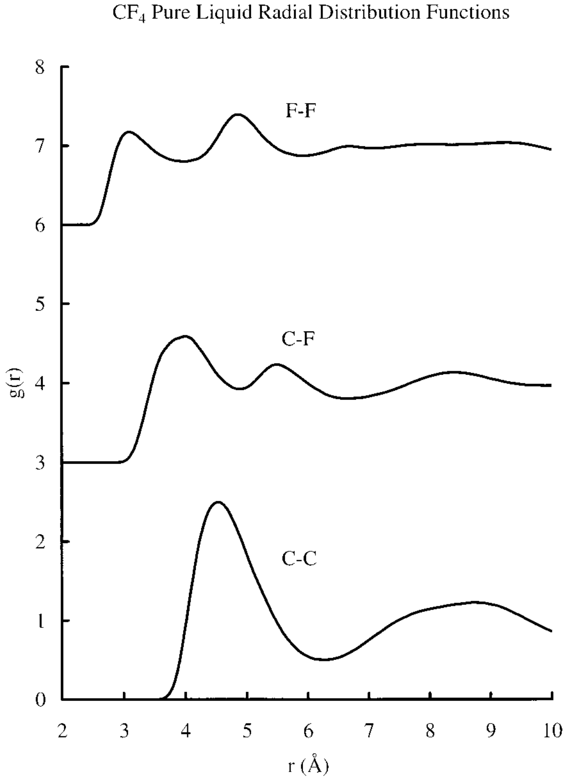

Figure 5. Intermolecular radial distribution functions for liquid CF_4 at −177 °C from MC simulations with the OPLS-AA force field. Successive curves are offset 3 units along the y axis.

Radial distribution functions generated for liquid CF_4 (−177 °C, 1.0 atm, $\rho = 1.86$ g cm^{-3}) with the OPLS-AA force field are presented in Figure 5. The first C−C maximum at 4.5 Å can be compared with literature values of 4.8 Å from another MC simulation at a similar state point (ca. −150 °C, 1 atm),[50] 4.6 Å from an MD simulation (−166 °C, 1.0 atm),[51] and 4.7 Å from a reverse-MC simulation based on neutron diffraction data in the supercritical regime at much lower density (97 °C, $\rho = 1.2$ g cm^{-3}).[48] The C−F maxima at 4.0 and 5.6 Å and the F−F maxima at 3.1 and 4.9 Å in Figure 5 also correspond to the maxima at 4.0, 5.5, 2.9, and 4.8 Å reported in the latter work.[48] Integration of the C−C rdf from the present MC simulation out to the first minimum at ca. 6.3 Å encompasses 13 neighbors, which matches the number of nearest neighbors calculated by Nose and Klein.[50] The first peak with an F−F maximum at ca. 3.0 Å in Figure 5 reflects the closest intermolecular atom−atom contacts for CF_4. Similarly, the MC results for C_3F_8 (−124

TABLE 6: Computed Densities and Heats of Vaporization from Pure Liquid Simulations at 1 atm

		density (g cm^{-3})		ΔH_{vap} (kcal mol^{-1})	
liquid	T (°C)	calcd	expt	calcd	expt
CF_4	−128.02	1.631 ± 0.005	1.608[a]	2.99 ± 0.01	3.00[b]
C_2F_6	−78.10	1.572 ± 0.003	1.590[c]	3.71 ± 0.02	3.86[d]
C_3F_8	−36.65	1.606 ± 0.004	1.600[e]	4.73 ± 0.04	4.69[e]
c-C_4F_8	−40.20	1.715 ± 0.003	1.753[f]	5.85 ± 0.06	5.63[g]
n-C_4F_{10}	0.00	1.581 ± 0.008	1.600[h]	5.45 ± 0.10	5.46[h]
c-C_5F_{10}	22.50	1.653 ± 0.003	1.637[i]	6.19 ± 0.16	6.31[i]
n-C_5F_{12}	25.00	1.597 ± 0.007	1.600[j]	6.52 ± 0.13	6.45[k]
$(CF_3)_2CFCF_2CF_3$	30.12	1.613 ± 0.004	1.631[j]	6.21 ± 0.06	6.49[i]
n-C_6F_{14}	25.00	1.681 ± 0.005	1.675[l]	7.86 ± 0.13	7.51[m]
$(CF_3)_2CF(CF_2)_2CF_3$	25.00	1.702 ± 0.006	1.718[n]	7.76 ± 0.11	7.50[m]
$(CF_3)_2(CF)_2(CF_3)_2$	20.00	1.779 ± 0.004	1.773[o]	7.96 ± 0.11	7.64[m]

[a] Average from refs 58 and 59. [b] Average from refs 60 and 61. [c] Average from refs 62 and 63. [d] Reference 64. [e] Reference 65. [f] Reference 66. [g] Reference 67. [h] Reference 68. [i] Reference 69. [j] Reference 70. [k] Average from refs 69 and 71. [l] Average from refs 72−74. [m] Reference 71. [n] Interpolated from ref 75. [o] Reference 76.

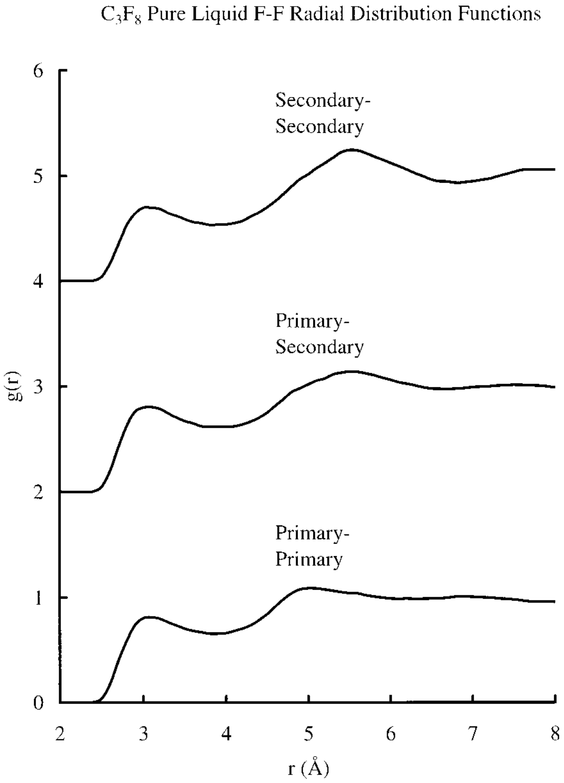

Figure 6. Intermolecular F−F radial distribution functions for liquid C_3F_8 at −124° C from MC simulations with the OPLS-AA force field. Successive curves are offset 2 units along the *y* axis.

°C, 0.5 atm) show F−F first maxima near 3.1 Å for primary (F on C1)−primary, primary−secondary (F on C2), and secondary−secondary interactions (Figure 6). These distances match the 3.2 Å F−F separation observed in a neutron diffraction study of liquid C_3F_8 and attributed to the closest intermolecular atom−atom contacts.[52]

Conclusions

The conformational characteristics and liquid-state properties of perfluoroalknaes have been explored in the course of the development of OPLS-AA force-field parameters. Though most prior force-field efforts have focused on linear perfluoroalkanes, the present work considered both ab initio and experimental data for linear and branched molecules. Ab initio LMP2/cc-pVTZ(-f)//HF/6-31G* results for the CCCC torsional energy profile of *n*-C_4F_{10} parallel prior ab initio and experimental results; they show enantiomeric pairs of gauche, ortho, and anti minima, with a low anti to trans barrier. The present LMP2 results for *n*-C_5F_{12} show a similar splitting into gauche, ortho, and anti minima, and the CCCF torsional energy profile of $(CF_3)_2CFCF_2CF_3$ is also split into three minima pairs.

Compound-specific OPLS-AA torsional parameters for *n*-C_4F_{10} and *n*-C_5F_{12} closely reproduce ab initio LMP2 torsional profiles and geometries, especially for the trans to gauche energy differences and for the torsional energy barriers. Compound-specific parameters for $(CF_3)_2CFCF_2CF_3$ also mimic well the ab initio torsional energy profile and geometries. However, the shallow ortho and anti minima for *n*-C_4F_{10} and *n*-C_5F_{12} from the ab initio calculations are not reproduced with the OPLS-AA compound-specific parameters. Generalized OPLS-AA parameters for all perfluoroalkanes were developed that match ab inito calculations within ca. 0.5 kcal/mol for the key conformational energy differences of the three reference compounds. Furthermore, the parameters have been tested in MC simulations for the pure liquids of eleven linear, branched, and cyclic perfluoroalkanes; the resultant densities and enthalpies of vaporization closely match experimental data. The computed peak positions in the intermolecular radial distribution functions for CF_4 and C_3F_8 also reproduce well results from prior computations and neutron diffraction data. The present results provide a solid basis for future MC and MD simulations of the fascinating chemistry of liquid perfluoroalkanes.

Acknowledgment. Gratitude is expressed to Dr. Julian Tirado-Rives and Prof. Kenneth B. Wiberg for helpful discussions; to Daniel J. Price, Melissa L. Plount, and Robert C. Rizzo for computational assistance; and to the National Institute of Allergy and Infectious Diseases for financial support.

Supporting Information Available: Ab initio LMP2/cc-pVTZ(-f)//HF/6-31G* energies vs torsional angle for *n*-C_4F_{10}, *n*-C_5F_{12}, and $(CF_3)_2CFCF_2CF_3$. This material is available free of charge via the Internet at http://pubs.acs.org.

References and Notes

(1) Chambers, R. D.; Sandford, G.; Shah, A. *Synth. Commun.* **1996**, *26*, 1861−1866.

(2) Zhu, D. W. *Synthesis* **1993**, 953−954.

(3) Chechik, V.; Crooks, R. M. *J. Am. Chem. Soc.* **2000**, *122*, 1243−1244.

(4) Rao, N. S.; Baker, B. E. Textile Finishes and Fluorosurfactants. In *Organofluorine Chemistry: Principles and Commercial Applications*; Banks, R. E., Smart, B. E., Tatlow, J. C., Eds.; Plenum: New York, 1994; pp 321−336.

(5) Guillevic, M. A.; Rocaboy, C.; Arif, A. M.; Horvath, I. T.; Gladysz, J. A. *Organometallics* **1998**, *17*, 707−717.

(6) DeSimone, J. M.; Maury, E. E.; Menceloglu, Y. Z.; McClain, J. B.; Romack, T. J.; Combes, J. R. *Science* **1994**, *265*, 356−359.

(7) Beckman, J. E. *Science* **1996**, *271*, 613−614.

(8) Johnston, K. P.; Harrison, K. L.; Clarke, M. J.; Howdle, S. M.; Heitz, M. P.; Bright, F. V.; Carlier, C.; Randolph, T. W. *Science* **1996**, *271*, 624−626.

(9) Gross, U.; Papke, G.; Rudiger, S. *J. Fluorine Chem.* **1993**, *61*, 11−16.

(10) Lowe, K. C. Properties and Biomedical Applications of Perfluorochemicals and Their Emulsions. In *Organofluorine Chemistry: Principles and Commercial Applications*; Banks, R. E., Smart, B. E., Tatlow, J. C., Eds.; Plenum: New York, 1994; pp 555−573.

(11) Miller, J. H., Jr.; Googe, J. M., Jr.; Hoskins, J. C. *Am. J. Ophthalmol.* **1997**, *123*, 705−707.

(12) Porter, T. R.; Xie, F.; Kricsfeld, A.; Kilzer, K. *J. Am. Coll. Cardiol.* **1995**, *26*, 33−40.

(13) Albinsson, B.; Michl, J. *J. Am. Chem. Soc.* **1995**, *117*, 6378−6379.

(14) Albinsson, B.; Michl, J. *J. Phys. Chem.* **1996**, *100*, 3418−3429.

(15) Neumann, F.; Teramae, H.; Downing, J. W.; Michl, J. *J. Am. Chem. Soc.* **1998**, *120*, 573−582.

(16) Smith, G. D.; Jaffe, R. L.; Yoon, D. Y. *Macromolecules* **1994**, *27*, 3166−3173.

(17) Okada, O.; Oka, K.; Kuwajima, S.; Tanabe, K. *Mol. Simul.* **1999**, *21*, 325−342.

(18) Chen, K.-H.; Walker, G. A.; Allinger, N. L. *J. Mol. Struct. (THEOCHEM)* **1999**, *490*, 87−107.

(19) Belyakov, A. V.; Haaland, A.; Shorokhov, D. J.; West, R. *J. Organomet. Chem.* **2000**, *597*, 87−91.

(20) Rosi-Schwartz, B.; Mitchell, G. R. *Phys. Scr.* **1995**, *T57*, 161−167.

(21) Rosi-Schwartz, B.; Mitchell, G. R. *Polymer* **1994**, *35*, 3139−3148.

(22) Holt, D. B.; Farmer, B. L. *Polymer* **1999**, *40*, 4667−4672.

(23) Holt, D. B.; Farmer, B. L. *Polymer* **1999**, *40*, 4673−4684.

(24) Rosi-Schwartz, B.; Mitchell, G. R. *Polymer* **1996**, *37*, 1857−1870.

(25) Rosi-Schwartz, B.; Mitchell, G. R. *Philos. Mag. B−Phys. Condens. Matter Stat. Mech. Electron. Opt. Magn. Prop.* **1996**, *73*, 153−161.

(26) Sprik, M.; Rothlisberger, U.; Klein, M. L. *J. Phys. Chem. B* **1997**, *101*, 2745−2749.

(27) Sprik, M.; Rothlisberger, U.; Klein, M. L. *Mol. Phys.* **1999**, *97*, 355−373.

(28) Jaffe, R. L.; Han, J.; Yang, L.; Yoon, D. Y. *Abstracts of Papers, Part 2*, 215th National Meeting of the American Chemical Society, Dallas, TX, March 29−April 2, 1998; American Chemical Society: Washington, DC, 1998; PMSE 201.

(29) Han, J.; Jaffe, R. L.; Yoon, D. Y. *Abstracts of Papers, Part 1*, 213th National Meeting of the American Chemical Society, San Francisco, CA, April 13−17, 1997; American Chemical Society: Washington, DC, 1997; COMP 294.

(30) Dixon, D. A.; Farnham, W. B.; Capobianco, P. J. *Int. J. Supercomput. Appl. High Perform. Comput.* **1990**, *4* (2), 134−149.

(31) Gough, C. A.; Debolt, S. E.; Kollman, P. A. *J. Comput. Chem.* **1992**, *13*, 963−970.

(32) Yamamoto, R.; Kitao, O.; Nakanishi, K. *Fluid Phase Equilib.* **1995**, *104*, 349−361.

(33) Cui, S. T.; Siepmann, J. I.; Cochran, H. D.; Cummings, P. T. *Fluid Phase Equilib.* **1998**, *146*, 51−61.

(34) Jorgensen, W. L.; Maxwell, D. S.; Tirado-Rives, J. *J. Am. Chem. Soc.* **1996**, *118*, 11225−11236.

(35) Cornell, W. D.; Cieplak, P.; Bayly, C. I.; Gould, I. R.; Merz, K. M., Jr.; Ferguson, D. M.; Spellmeyer, D. C.; Fox, T.; Caldwell, J. W.; Kollman, P. A. *J. Am. Chem. Soc.* **1995**, *117*, 5179−5197.

(36) Jorgensen, W. L. *BOSS*, version 4.2; Yale University: New Haven, CT, 2000.

(37) *Jaguar*, version 3.5; Schrodinger, Inc.: Portland, OR, 1998.

(38) Parra, R. D.; Zeng, X. C. *J. Fluorine Chem.* **1997**, *83*, 51−60.

(39) Muir, M.; Baker, J. *Mol. Phys.* **1996**, *89*, 211−237.

(40) Parra, R. D.; Zeng, X. C. *J. Phys. Chem. A* **1998**, *102*, 654−658.

(41) Smith, J. H.; Pace, E. L. *J. Phys. Chem.* **1969**, *73*, 2368−2372.

(42) Murphy, R. B.; Beachy, M. D.; Friesner, R. A.; Ringnalda, M. N. *J. Chem. Phys.* **1995**, *103*, 1481−1490.

(43) Friesner, R. A.; Murphy, R. B.; Beachy, M. D.; Ringnalda, M. N.; Pollard, W. T.; Dunietz, B. D.; Cao, Y. X. *J. Phys. Chem. A* **1999**, *103*, 1913−1928.

(44) Tirado-Rives, J. *Fit*, version 1.0; Yale University: New Haven, CT, 2000.

(45) Metropolis, N.; Rosenbluth, A. W.; Rosenbluth, M. N.; Teller, A. H. *J. Chem. Phys.* **1953**, *21*, 1087−1092.

(46) Jorgensen, W. L. Monte Carlo Simulations for Liquids. In *Encyclopedia of Computational Chemistry*; Schleyer, P. v. R., Ed.; Wiley: New York, 1998; Vol. 3, pp 1754−1763.

(47) Rizzo, R. C.; Jorgensen, W. L. *J. Am. Chem. Soc.* **1999**, *121*, 4827−4836.

(48) Waldner, I.; Bassen, A.; Bertagnolli, H.; Todheide, K.; Strauss, G.; Soper, A. K. *J. Chem. Phys.* **1997**, *107*, 10667−10674.

(49) Mack, H. G.; Dakkouri, M.; Oberhammer, H. *J. Phys. Chem.* **1991**, *95*, 3136−3138.

(50) Nose, S.; Klein, M. L. *J. Chem. Phys.* **1983**, *78*, 6928−6939.

(51) Brode, S.; McDonald, I. R. *Mol. Phys.* **1988**, *65*, 1007−1012.

(52) Johnson, K. A.; Howells, W. S. *J. Phys.-Condes. Matter* **1999**, *11*, 9239−9248.

(53) Dixon, D. A. *J. Phys. Chem.* **1992**, *96*, 3698−3701.

(54) Campos-Vallette, M.; Rey-Lafon, M. *J. Mol. Struct.* **1984**, *118*, 245−255.

(55) Campos-Vallette, M.; Rey-Lafon, M. *J. Mol. Struct.* **1983**, *101*, 23−45.

(56) Piaggio, P.; Francese, P. G.; Masetti, G.; Dellepiane, G. *J. Mol. Struct.* **1975**, *26*, 421−428.

(57) Kollman, P. A. University of California, San Francisco, CA. Personal communication, 1994.

(58) Terry, M. J.; Lynch, J. T.; Bunclark, M.; Mansell, K. R.; Staveley, L. A. K. *J. Chem. Thermodyn.* **1969**, *1*, 413−424.

(59) Knobler, C. M.; Pings, C. J. *J. Chem. Eng. Data* **1965**, *10*, 129−130.

(60) Boublik, T. *Collect. Czech. Chem. Commun.* **1972**, *37*, 2499−2506.

(61) Maslov, Y. P.; Maslov, P. G. *J. Gen. Chem. USSR (Engl. Transl.)* **1966**, *36*, 398−402.

(62) Swarts, F. *Bull. Soc. Chim. Belg.* **1933**, *42*, 114−118.

(63) Ruff, O.; Bretschneider, O. *Z. Anorg. Allg. Chem.* **1933**, *210*, 173−183.

(64) CRC Handbook of Chemistry and Physics. http://www.knovel.com (accessed May 2000), path: Knovel/CRC/CRC Handbook of Chemistry and Physics/Result for c2f6/Section 6: Fluid Properties/Enthalpy of Vaporization.

(65) Brown, J. A. *J. Chem. Eng. Data* **1963**, *8*, 106−108.

(66) Martin, J. J. *J. Chem. Eng. Data* **1962**, *7*, 68−72.

(67) Bambach, G. *Kaeltetechnik* **1956**, *8*, 334−339.

(68) Brown, J. A.; Mears, W. H. *J. Phys. Chem.* **1958**, *62*, 960−962.

(69) Barber, E. J.; Cady, G. H. *J. Phys. Chem.* **1956**, *60*, 504−505.

(70) Burger, L. L.; Cady, G. H. *J. Am. Chem. Soc.* **1951**, *73*, 4243−4246.

(71) Basarova, P.; Svoboda, V. *Fluid Phase Equilib.* **1991**, *68*, 13−34.

(72) Brice, T. J.; Coon, R. I. *J. Am. Chem. Soc.* **1953**, *75*, 2921−2925.

(73) Dunlap, R. D.; Murphy, C. J., Jr.; Bedford, R. G. *J. Am. Chem. Soc.* **1958**, *80*, 83−85.

(74) Kennan, R. P.; Pollack, G. L. *J. Chem. Phys.* **1988**, *89*, 517−521.

(75) Stiles, V. E.; Cady, G. H. *J. Am. Chem. Soc.* **1952**, *74*, 3771−3773.

(76) Miller, W. T. Preparation of Halo Aliphatic Compounds. U. S. Patent 2,716,141, Aug 23, 1955.